

See discussions, stats, and author profiles for this publication at: <https://www.researchgate.net/publication/264462431>

Effects of Radiation and Temperature on Iodide Sorption by Surfactant-Modified Bentonite

ARTICLE *in* ENVIRONMENTAL SCIENCE AND TECHNOLOGY · AUGUST 2014

Impact Factor: 5.33 · DOI: 10.1021/es501661z · Source: PubMed

CITATIONS

2

READS

35

5 AUTHORS, INCLUDING:



Sungwook Choung

Korea Basic Science Institute KBSI

15 PUBLICATIONS 26 CITATIONS

[SEE PROFILE](#)



Min Gyu Kim

Pohang University of Science and Technology

151 PUBLICATIONS 5,121 CITATIONS

[SEE PROFILE](#)



Wooyong Um

Pacific Northwest National Laboratory

91 PUBLICATIONS 799 CITATIONS

[SEE PROFILE](#)

Effects of Radiation and Temperature on Iodide Sorption by Surfactant-Modified Bentonite

Sungwook Choung,^{†,V} Minkyung Kim,[†] Jung-Seok Yang,[§] Min-Gyu Kim,^{||} and Wooyong Um^{*,†,⊥}

[†]Division of Advanced Nuclear Engineering, Pohang University of Science and Technology (POSTECH), 77 Chongam-ro, Nam-gu, Pohang 790-784, Republic of Korea

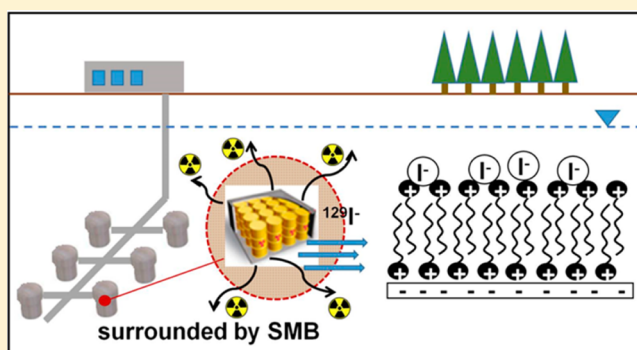
[§]Environmental Research Group, Korea Institute of Science & Technology (KIST), 679 Saimdang-ro, Gangneung 210-340, Republic of Korea

^{||}Pohang Accelerator Laboratory (PAL), 77 Chongam-ro, Nam-gu, Pohang 790-784, Republic of Korea

[⊥]Energy and Environment Directorate, Pacific Northwestern National Laboratory (PNNL), 902 Battelle Blvd., P7-54, Richland, Washington 99354, United States

Supporting Information

ABSTRACT: Bentonite, which is used as an engineered barrier in geological repositories, is ineffective for sorbing anionic radionuclides because of its negatively charged surface. This study modified raw bentonite using a cationic surfactant (i.e., hexadecyltrimethylammonium [HDTMA]-Br) to improve its sorption capability for radioactive iodide. The effects of temperature and radiation on the iodide sorption of surfactant-modified bentonite (SMB) were also evaluated under alkaline pH condition similar to that found in repository environments. Different amounts of surfactant, equivalent to the 50, 100, and 200% cation-exchange capacity of the bentonite, were used to produce the HDTMA-SMB for iodide sorption. The sorption reaction of the SMB with iodide reached equilibrium rapidly within 10 min regardless of temperature and radiation conditions. The rate of iodide sorption increased as the amount of the added surfactant was increased and nonlinear sorption behavior was exhibited. However, high temperature and γ -irradiation (^{60}Co) resulted in significantly ($\sim 2\text{--}10$ times) lower iodide K_d values for the SMB. The results of FTIR, NMR, and XANES spectroscopy analysis suggested that the decrease in iodide sorption may be caused by weakened physical electrostatic force between the HDTMA and iodide, and by the surfactant becoming detached from the SMB during the heating and irradiation processes.



INTRODUCTION

Anthropogenic radioactive iodine is generated by nuclear fuel reprocessing, atomic bomb tests, and nuclear accidents such as those experienced at Chernobyl and Fukushima.^{1–4} Radioactive iodine can be accumulated in the human thyroid gland, which results in increased incidence of hyperthyroidism, goiter, and thyroid cancer in humans.^{5,6} Among the radioiodine isotopes (e.g., $^{125}/^{129}/^{131}\text{I}$), ^{129}I is of greatest environmental concern because of its long half-life of 1.6×10^7 yr, and its high mobility due to relatively high solubility.¹ The mobility of radioactive iodine is strongly controlled by iodine speciation under certain pH-Eh conditions.^{7–9} Dominant iodine species are anionic forms, such as iodide (I^-), iodate (IO_3^-), and organo iodine in the natural environment.^{8,9} Iodide, which is mainly found under reducing conditions in deep radioactive waste repositories,¹⁰ possesses a low sorption affinity for geologic media because the surfaces of many minerals are mostly negatively charged at circumneutral pH condition.¹¹ Therefore, iodide is one of the most difficult elements in radioactive wastes to control using

sorption and retardation by minerals found in the pathway from the deep geological repository to nearby humans and environments.

Multiple barrier systems have been used to prevent release of radionuclides from geological repositories to the surrounding environment. Bentonite has been regarded as a qualified backfill material for engineered barriers in radioactive waste disposal sites. It is characterized by a high swelling property, a high sorption capacity for cationic radionuclides, and low permeability.^{12,13} However, bentonite is ineffective for sorbing anionic radionuclides such as iodine species,^{12,13} because it has both a permanently negatively charged surface like other aluminosilicate minerals and a pH-dependent negative surface charge caused by deprotonation of the surface hydroxyl group under

Received: April 3, 2014

Revised: July 31, 2014

Accepted: August 4, 2014

Published: August 4, 2014



high pH conditions. Therefore, surface modification of bentonite has been proposed to enhance its sorption capacity for anionic radionuclides. For example, surfactant-modified bentonite (SMB) was developed by converting the surface charge of bentonite from negative to positive using a cationic surfactant.^{14–16} Ion exchange with alkyl ammonium is the preferred method because of the high affinity of alkyl ammonium for clay.¹⁷ In particular, long C-chain organic surfactant (e.g., hexadecylpyridinium- [HDPy⁺] and benzethonium- [BE⁺])-modified bentonite exhibited great sorption distribution coefficients for iodide.¹²

Although the SMB exhibits significantly increased iodide sorption capacity, the impact of heat and radiation on iodide sorption by SMB must be evaluated at the geological repository, because (1) radiation increases the surface temperature of radioactive waste containers to ~75–120 °C, and consequently, the engineered barrier, which is placed outside the containers, could be exposed to comparatively high temperatures (e.g., 40–93 °C);¹³ and (2) radiation destroys the clay mineral structure by breaking the chemical bonding of Al–O and Si–O under a 9.2×10^5 Gy dose at 95 °C.¹⁸ The cumulative annual gamma dose of 6×10^6 Gy was projected from nuclear waste glasses at the Savannah River Plant.¹⁹ Although a few studies have conducted iodide sorption experiments for SMB under various temperature conditions,^{13,20} the radiation and temperature effects on iodide sorption to SMB were seldom studied.

The main goal of this study was to address the potential use of SMB as a material for a final engineered barrier to prevent the release of radioactive iodide under similar subsurface conditions within and from underground geological repositories. Hexadecyltrimethylammonium (HDTMA)-SMB was used in this study, because its iodide sorption capacity is greater than HDPy-SMB at high temperature.¹² Specific objectives of our research were to evaluate the temperature and radiation effects on iodide sorption by the HDTMA-SMB and elucidate the potential sorption mechanism for iodide on the HDTMA-SMB.

MATERIALS AND METHODS

Materials. Bentonite and HDTMA-Br were obtained from Sigma-Aldrich (St. Louis, MO). The chemical composition of the bentonite reported by the supplier was SiO₂ (63.02 wt.%), Al₂O₃ (21.1 wt.%), Fe₂O₃ (3.25 wt.%), FeO (0.35 wt.%), MgO (2.67 wt.%), Na₂O/K₂O (2.57 wt.%), and CaO (0.65 wt.%). The ammonium acetate method²¹ was used to determine the cation-exchange capacity (CEC) of the bentonite. Briefly, 1 g of bentonite was saturated with 30 mL of 1 M ammonium acetate solution for 30 min. The bentonite slurry was centrifuged at 2000 rpm for 15 min, and then supernatant was collected for exchangeable cation analyses. The saturation and centrifugation procedures were repeated three times, and the major cations (K, Na, Ca, and Mg) were analyzed using inductively coupled plasma atomic emission spectrometry (ICP-AES). The total CEC value of the bentonite (meq/100 g) was determined by the summation of major cations' equivalence concentrations divided by the mass of bentonite.

Potassium iodide (KI) was purchased from Junsei (Tokyo, Japan) to prepare an iodide stock solution for the sorption experiments. Stable iodide (¹²⁷I⁻) was used as surrogate for radioactive iodide (¹²⁹I⁻) in this study. Two concentrations of iodide stock solution were individually prepared by adding 26.2 mg of KI to 1 L of Milli-Q water (EMD Millipore Corp.,

Billerica, MA) to derive 0.15 mM of solution, and 392.5 mg of KI to 150 mL of Milli-Q water to prepare 15 mM of solution.

Synthesis and Characterization of SMB. The bentonite was modified to enhance its iodide sorption capacity by reacting the cationic surfactant of HDTMA-Br onto the bentonite surface. Three HDTMA-SMBs were synthesized using equivalent amounts of HDTMA-Br corresponding to 50, 100, and 200% of the CEC of bentonite, hereafter referred to as the 50-, 100-, and 200-SMB, respectively. Approximately 1.9, 3.7, and 7.4 g of HDTMA-Br was dissolved in 500 mL of Milli-Q water, and stirred for 30 min at 60 °C. After 10 g of the bentonite was added to each HDTMA-Br solution, the bentonite was consistently mixed for 6 h at 60 °C. The reacted bentonite was repeatedly washed with Milli-Q water until no bromide was found in the washings. The supernatant was decanted after centrifugation, and the residue was oven-dried at 105 °C overnight. The HDTMA-SMB was pulverized using a mortar and pestle to isolate the <100 μm sized particles, which were stored in a desiccator before the sorption experiments.

The organic carbon fraction of the SMB (f_{oc}) was analyzed to compare the amount of HDTMA loaded on the bentonite with the amount of added surfactant. The f_{oc} was quantified by coulometric CO₂ detection (CMS015, UIC Inc., IL) after combustion at 950 °C under pure oxygen conditions. In addition, X-ray diffraction (XRD) and scanning-electron microscopy-energy dispersive spectroscopy (SEM-EDS) analyses were conducted to characterize the SMB and the raw bentonite material. The basal spacing (d_{001}) of the raw bentonite and SMB was determined by XRD (D/Max-2500/PC, Rigaku) using Cu K α radiation at 40 kV and 25 mA. The step-scanning technique was used to obtain XRD patterns from 2 to 12 degrees 2 θ with a fixed step size of 0.03 degree 2 θ . The XRD peak intensity was determined using JADE v9.3 software (JADE Inc., Livermore, CA). The basal spacing (d_{001}) of the raw bentonite and SMB was computed using Bragg's law ($2ds\sin\theta = n\lambda$, where the interlayer distance of d [nm] corresponds to basal spacing; 2 θ [°] denotes scattered angle; n is an integer, and λ is the X-ray radiation wavelength [$\lambda = 1.7890$ Å]). A Hitachi Su-70 SEM equipped with an EDAX Pegasus XM4 EDS was used to characterize the morphologies of the raw bentonite and SMB, and to investigate iodine distribution onto the SMB surface after sorption experiments. The SMB sample was coated with osmium, and the operating conditions of the electron microprobe accelerating voltage, 15 kV under vacuum 10^{-3} Pa, were preserved during analysis.

Iodide Sorption Experiments. Iodide sorption experiments were conducted to determine the equilibrium time (or reaction rate), sorption capabilities, and nonlinearities for raw bentonite and HDTMA-SMB samples. The equilibration time was determined by kinetic sorption experiments for 24 h using the bentonite and 100-SMB. Based on the measured equilibrium time, the equilibrium sorption isotherms were developed for the SMB samples to determine the sorption capabilities and nonlinearities. Batch techniques were used for all sorption experiments in this study.

Approximately 0.5 and 0.1 g of raw bentonite and SMB were individually added to the preweighed glass vials for batch experiments. Up to ~25 and 10 mL of prepared background solution (0.001 M NaNO₃ in Milli-Q water) was then added to the sorption vials of the bentonite and HDTMA-SMB, respectively. The ratio of solid to solution was optimized by prescreening iodide sorption experiments. Each sorbent was presaturated for 24 h with the background solution prior to

injecting iodide into the solution. The volume of iodide stock solution injected into the batches was adjusted to obtain approximately 300 $\mu\text{g/L}$ –600 mg/L of initial target iodide concentrations. The batch vials were immediately sealed using Teflon-lined lids after iodide injection. Solid-free control vials were also prepared in parallel with the sorption batches to determine the initial total mass and any loss of iodide mass by the test vials during the batch experiment. All sorption and control vials were prepared in duplicate, stored in a dark, and rotated at 130 rpm during the experimental period. The sorption vials were centrifuged after the sorption experiments, and aqueous phases were separated to analyze the dissolved iodide concentration (C_w [$\mu\text{g/L}$]) measured using an ICP mass spectrometer (ICP-MS; PerkinElmer NexION 300D). The sorbed iodide concentration (C_s [$\mu\text{g/kg}$]) was determined by mass balance. The initially added masses of iodide was approximately $< \pm 10\%$ different from the experimentally determined mass in control vials.

The sorption experiments were also performed to evaluate the effects of temperature and radiation on the iodide sorption by the HDTMA-SMB. Different temperature conditions (25, 60, and 90 °C) were controlled by a water bath during the sorption reaction, and the initial iodide concentration was adjusted to $\sim 300 \mu\text{g/L}$ as the lowest concentration range in this study. In addition, the HDTMA-SMB samples were irradiated with a γ -dose of approximately 10^6 Gy using a ^{60}Co -energy source at 25 °C and were used for iodide sorption experiments. The initial concentration range was adjusted to 300 $\mu\text{g/L}$ –600 mg/L to develop the sorption isotherms for the irradiated SMB samples.

Characterization of SMB after Irradiation. Nuclear magnetic resonance (NMR) spectrometry analysis was conducted to determine the change in the structural properties of the bentonite and SMB after irradiation (i.e., comparison of bentonite, irradiated bentonite, 200-SMB, and irradiated 200-SMB). Both solid-state magic-angle spinning $^{27}\text{Al-NMR}$ and ^{29}Si NMR spectra were obtained at a Larmor frequency of 104.26 and 79.48 MHz, respectively, using a 400-MHz Avance II+ Bruker solid-state NMR spectrometer. Sample spinning was conducted at 13 kHz with 0.5-s delay time for $^{27}\text{Al-NMR}$ spectra, and at 10 kHz with 120-s delay time for ^{29}Si NMR spectra.

Fourier transform infrared spectroscopy (FTIR) spectra were obtained to evaluate the change of chemical bonds between different samples after irradiation and/or iodide sorption: raw bentonite, irradiated bentonite, 200-SMB, irradiated 200-SMB, 200-SMB sorbed by iodide, 200-SMB irradiated after iodide sorption, and 200-SMB sorbed by iodide after irradiation. For the FTIR analyses, the iodide-SMB sorption experiments were conducted at comparatively high initial concentration ($> \sim 30 \text{ mg/L}$). A Hyperion 3000 microscope installed on a Vertex 80 spectrometer (Bruker Optics, Germany) with a Ge-on-KBr beam splitter was used for the FTIR spectra. The microscope was equipped with a Ge-attenuated total reflectance objective lens (ATR 20X) and a liquid N₂-cooled mercury–cadmium–telluride detector. This instrument was continuously purged with dry N₂ gas to minimize the background absorption by water vapor and carbon dioxide in the atmosphere. For the bentonite and HDTMA-SMB samples, 256 scans were used with KBr pellets to measure the spectral range from 350 to 4000 cm^{-1} .

X-ray absorption near edge structure (XANES) spectroscopy was used to determine the iodine oxidation state change. Iodine

K-edge (33.169 keV) XAFS spectra were collected at beamline BL10C of the Pohang Light Source (PLS-II) in the Pohang Accelerator Laboratory (PAL), South Korea under a ring current of 100 mA at 3.0 GeV. High intensity X-ray photons of multipole wiggler source provided a monochromatic X-ray beam through a liquid-nitrogen cooled Si (111) double-crystal monochromator. For XAFS sample preparation, sieved fine powder samples were uniformly dispersed with a proper thickness on the polyimide film. Potassium iodate (KIO₃) and iodide (KI) were used for iodine reference peaks. Reference material (KI) was placed in front of the last reference ion chamber for energy calibration to compensate for the energy shift. Data reductions of the collected spectra to normalize XANES was performed through the standard XAFS procedure using the UWXAFS program.²² The 200% SMB and 10^6 Gy irradiated 200% SMB after iodide adsorption samples were measured to identify the iodine oxidation state change by XANES analysis.

RESULTS AND DISCUSSION

SMB Characterization. The measured CEC was 101.8 mequiv/100 g for the raw bentonite used in this study, which is a typical value supported by other bentonite studies.^{23–25} The f_{oc} values of the SMB increased to 0.11, 0.18, and 0.21 g C g⁻¹ for the 50-, 100-, and 200-SMB, respectively (Figure S1 in Supporting Information (SI)), corresponding to the increase in the amount of surfactant added from 50 to 200% of the bentonite CEC. The surfactant adsorbed completely by the 50-SMB showing approximately 95% sorption efficiency compared to the injected HDTMA. In contrast, the surfactant sorption efficiency decreased to $\sim 80\%$ for the 100-SMB, and $\sim 50\%$ for the 200-SMB. The cationic surfactant could interact with the active sorption sites of the bentonite at external surfaces, broken edges, and interlamellar spaces.^{26–28} Correspondingly, the XRD patterns indicated that the interlayer distance of the SMB expanded with the increased amount of surfactant added to the bentonite (Figure 1), because the arrangement of HDTMA formed monolayers, bilayers, and paraffin complexes in the interlamellar region.²⁹ Although the basal spacing of 1.59

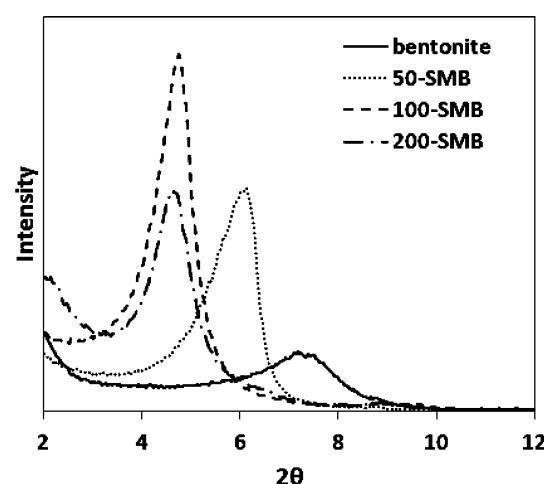


Figure 1. XRD patterns of the raw bentonite and the 50-, 100-, and 200-SMB. The basal spacing of individual SMB sample was derived from the Bragg's law. The basal spacing increased with the increasing amount of surfactant added (50-SMB $<$ 100-SMB \leq 200-SMB), indicating that arrangements of surfactant formed layers in the interlamellar region.

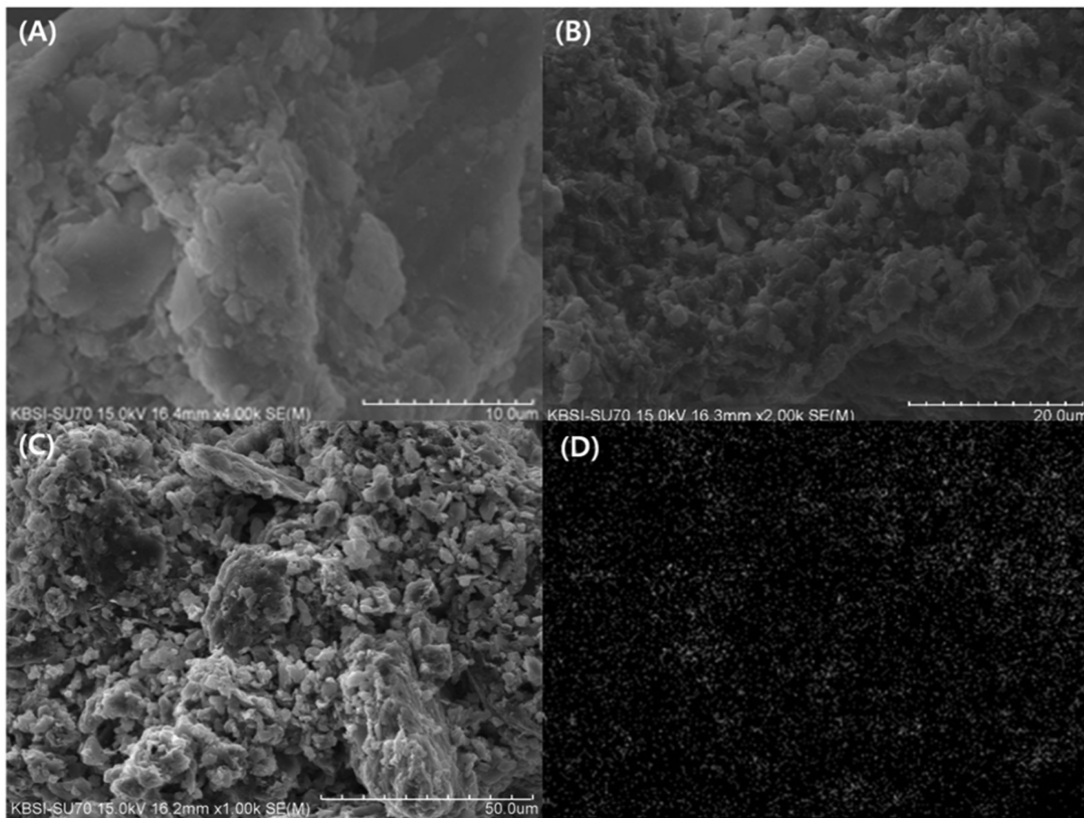


Figure 2. SEM images of (A) the raw bentonite, (B) 200-SMB, and (C) 200-SMB after iodide sorption reaction, and (D) the good distribution of iodide (green) sorbed by 200-SMB in Figure 2C.

nm for the 50-SMB showed a slight increase over the $d_{001} = 1.49$ nm of the raw bentonite, a significant increase in the basal spacing was observed between 50- and 100-SMB. However, the change in basal spacing between the 100- and 200-SMB was negligible— $d_{001} = 2.02$ and 2.05 nm, respectively.

The surface morphologies of the raw bentonite and 200-SMB were illustrated by SEM analysis (Figure 2). The 200-SMB shows significant changes in surface morphology, compared to the raw bentonite. The surface was quite smooth for the raw bentonite, but became rougher after intercalation of the cationic surfactant. In addition, numerous small and aggregated morphologies were clearly observed in the micrograph for the 200-SMB, unlike the raw bentonite. The SEM-EDS-derived element peaks showed the existence of carbon in the SMB sample (SI Figure S2), suggesting the intercalation of HDTMA into the bentonite structure.

Kinetic Iodide Sorption. The kinetic sorption experiments were performed at the relatively low end of the dissolved iodide concentrations within the range used for isotherm development (i.e., $C_w \approx 100 \mu\text{g/L}$), because sorption reactions are site-limited and strongly dependent on the diffusion processes.³⁰ The final pH of ~ 8 was applied to represent a typical alkaline condition of groundwater environments in geological repositories such as the SFR in Sweden,³¹ the VLJ in Finland,³² and the Gyeongju site in Korea.³³ The equilibration time of iodide sorption on the bentonite and 100-SMB was also evaluated under high-temperature and irradiated conditions.

The HDTMA-SMB reacted rapidly with iodide within <10 min (Figure 3), while iodide sorption was negligible for the raw bentonite (not shown here). The iodide sorption rate by the SMB was not quantified in this study, because experimental

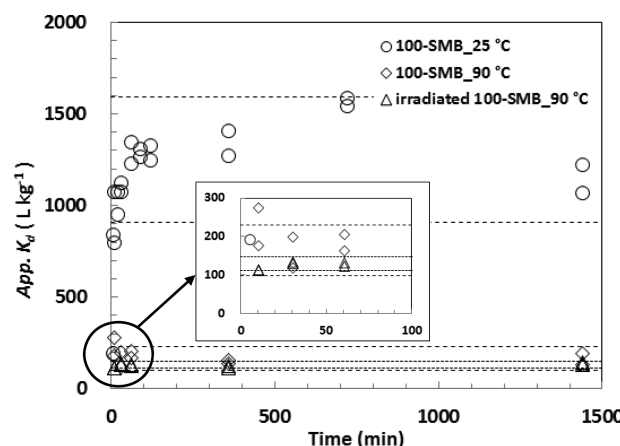


Figure 3. Equilibrium time measurements for 100-SMB and irradiated 100-SMB under different temperature conditions (25 and 90 °C). The dashed lines indicate the 2-sigma of average K_d values measured after 10 min under each condition.

errors were high in duplicate for the data points measured at very short initial reaction times. High sorption uncertainties may be caused by different diffusion rates, depending on the vigorous-mixing scheme for each batch at the beginning of the sorption experiments. Qualitative observation from relatively longer reaction time indicated that the sorption reaction was relatively faster at a high temperature condition of 90 °C than at ambient temperature. Irradiation had no significant effect on the equilibration time for the iodide-SMB system. Therefore, based on the kinetic results, we determined that 24 h is

sufficient time for the generation of equilibrated iodide sorption isotherms using SMB.

Iodide Sorption Isotherms. The measured sorption isotherms of iodide on the HDTMA-SMB (Figure 4) were

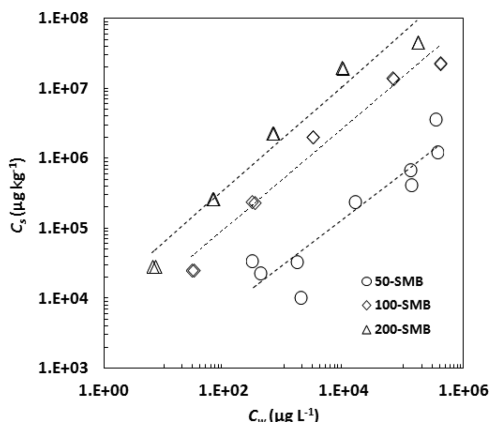


Figure 4. Iodide sorption isotherms for the 50-, 100-, and 200-SMB at 25 °C. The dashed lines indicate the Freundlich isotherm fits.

illustrated using the Freundlich model: $C_s = K_f C_w^n$ where K_f [$(\mu\text{g}/\text{kg})/(\mu\text{g}/\text{L})^n$] and n [−] are the Freundlich sorption coefficient and exponent, respectively. The Freundlich n values ranging from 0.65–0.75 (Table 1) indicated that all isotherms

Table 1. Freundlich Isotherm Parameters for Iodide Sorption on the Unirradiated and Irradiated SMB Samples^a

samples	K_f [$(\mu\text{g}/\text{kg})/(\mu\text{g}/\text{L})^n$]	n [-]	r^2
Unirradiated			
50-SMB	330	0.65	0.86
100-SMB	3400	0.73	0.97
200-SMB	11 000	0.75	0.96
Irradiated			
50-SMB	na	na	na
100-SMB	1400	0.73	0.96
200-SMB	2100	0.82	0.93

^aThe measured iodide initial concentration range was $C_w \approx 10 \mu\text{g}/\text{L}$ –400 mg/L. All sorption experiments were conducted at room temperature (25 °C) under pH 8 condition. na: not available.

for the SMB were nonlinear with concave downward shape (i.e., $n < 1$). The type of observed isotherms reflects that the sorption efficiency decreases more with increasing sorbate concentrations.³⁴ Therefore, the iodide sorption isotherms for the SMB samples showed significantly concentration-dependent behavior at the measured concentration range of $\approx 10 \mu\text{g}/\text{L}$ to 400 mg/L. These results imply greater sorption capacities of the SMB at lower dissolved iodide concentrations.

The iodide sorption increased with the increase in the added amount of surfactant. The sorption distribution coefficient (K_d) values were computed by the determined Freundlich sorption model to compare the iodide sorption capabilities of each SMB at identical concentration under pH 8. The K_d s showed approximately 70, 970, and 3600 L/kg for the 50-, 100-, and 200-SMB, respectively, at $C_w = 100 \mu\text{g}/\text{L}$. The iodide K_d values for natural organic matter (NOM) reported from other literatures were used to compare the sorption capability of the HDTMA-SMB, because (1) it is well-known that iodide is strongly assimilated by NOM through C–I bond forma-

tion,^{8,35,36} and (2) organic surfactant was used in this study. The iodide sorption behavior on an organic surfactant is expected to be similar to the sorption by NOM due to abundant carbon atoms as major element in organic surfactant. The iodide K_d values of the synthetic black carbon material³⁰ and humic acid extracted from contaminated surface soil³⁷ at the Savannah River Site were ~ 220 and 2500 L/kg, respectively, at an initial iodide concentration of 100 $\mu\text{g}/\text{L}$ under neutral pH conditions. These results indicated that the 200-SMB has a comparatively greater sorption capacity for iodide than the NOM. The high iodide sorption capabilities of the 200-SMB observed in this study suggested that the 200-SMB could be the most effective sorbent for removing radioactive iodide even in alkaline and reducing groundwater conditions (e.g., similar to those found in a deep geological repository).

Although the 100-SMB exhibited approximately 14 times greater iodide sorption than the 50-SMB, the relative sorption increase was only 3.7 times for the 200-SMB compared to the 100-SMB (i.e., 50-SMB \ll 100-SMB $<$ 200-SMB). These results implied that the iodide sorption by SMB may be related to the intercalated HDTMA in the interlamellar region of the bentonite more than those sorbed on other sites, because the increase of basal spacing was nearly maximized for the 100-SMB among the SMB samples used in this study.

Effects of Radiation and Temperature on Iodide Sorption.

The temperature effect on iodide sorption was evaluated at the lowest initial iodide concentration used ($\sim 300 \mu\text{g}/\text{L}$). Iodide sorption by the 200-SMB declined with increasing temperature, showing approximately ~ 10 times lower K_d ($= 470 \text{ L/kg}$) measured at 90 °C compared to the K_d ($= 4200 \text{ L/kg}$) at 25 °C (SI Figure S3). The decrease in iodide sorption could reflect the increase of entropy at high temperature in the solid, so the iodide prefers to remain in the solution phase. A previous study found that the sorptive attraction forces between the anion and sorbent may become physically weaker at high temperatures.²⁶ These temperature effects could not be caused by structural changes of the SMB, because the prior study for the increasing temperature effects on structural changes of HDTMA-SMB found no noticeable structure changes (e.g., basal spacing) for the HDTMA-SMB at high temperatures up to 180 °C.³⁸

The sorption capabilities for the SMB samples also decreased after irradiation (Figure 5). The iodide K_d values for the irradiated samples were ~ 2 –10 times lower than those of the unirradiated samples. In particular, the high temperature resulted in an additional sorption decrease for irradiated 200-SMB sample (Figure 5b). The NMR and FTIR spectra were measured, and the absolute individual peak areas were compared to evaluate the structural and chemical changes in the raw bentonite as well as the decrease in iodide sorption for the 200-SMB after the irradiation process. The ²⁷Al- and ²⁹Si NMR spectra exhibited the aluminum phyllosilicate structure of bentonite;²⁹ Al and Si were present in the octahedral and tetrahedral sheets (Figure 6). No significant structural changes were observed for the irradiated bentonite in the NMR spectra; the chemical shift and intensity of the NMR peaks between unirradiated and irradiated samples were nearly identical. However, the decrease in the FTIR band intensity of the peaks at around 1,000–1050 cm^{-1} (representing Si–O stretching and Si–O–Si bond) and at 465 cm^{-1} (representing Si–O–Al bending vibration) implies the broken (or weaken) structures of bentonite after gamma-irradiation (Figure 7a).

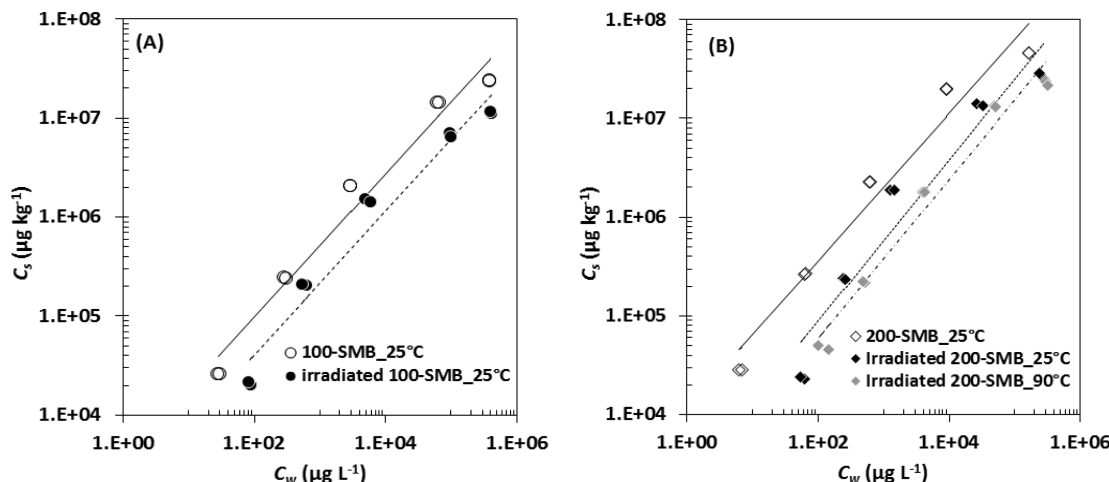


Figure 5. Comparison of the iodide sorption isotherms between unirradiated and irradiated SMB samples at 25 and 90 °C: (A) 100-SMB and (B) 200-SMB. The initial iodide concentration range was adjusted to 300 μg/L–600 mg/L for the sorption isotherm development. The solid and dashed lines represent the Freundlich fits for unirradiated and irradiated SMB, respectively.

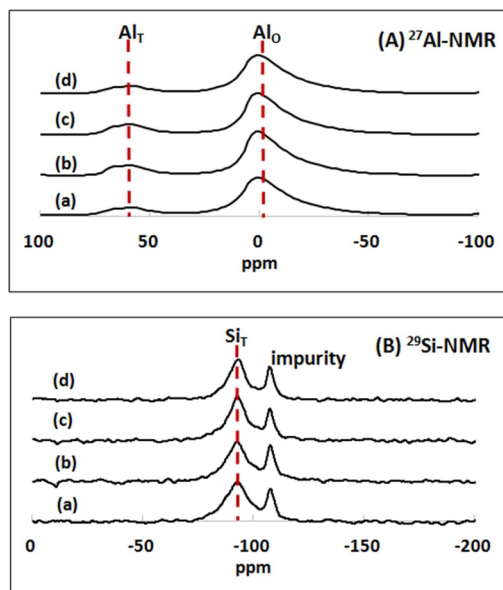


Figure 6. (A) ^{27}Al -NMR and (B) ^{29}Si NMR spectra for (a) bentonite, (b) irradiated bentonite, (c) 200-SMB, and (d) irradiated 200-SMB. The subscripts of $(\text{Al}/\text{Si})_T$ and Al_O represent tetrahedral and octahedral sites, respectively. The irradiated samples were irradiated using 10^6 Gy of ^{60}Co .

These band intensities declined more for the 200-SMB than for the raw bentonite, because the organic surfactant occupied the bentonite surfaces.³⁹ The pair of bands at 2850 and 2920 cm^{-1} —corresponding to symmetric and asymmetric stretching vibrations of the aliphatic C–H in CH_2 and CH_3 groups, respectively—supports the presence of intercalated surfactant in the SMB.⁴⁰ Interestingly, the irradiated HDTMA-SMB showed the increase in band intensity for the peaks of Si–O and Si–O–Al bonding in the comparison of the unirradiated samples (Figure 7b and c). It is believed that the surfactant was removed from the bentonite during the γ -irradiation process. These results could be supported by an ~5% average decrease in the measured f_{oc} values for the irradiated SMB samples compared to the unirradiated HDTMA-SMB samples (SI Figure S1). Therefore, the decreased iodide sorption by irradiation might result from detachment of the surfactant

from the SMB, although it could be also affected by the broken structures of the bentonite during γ -irradiation. The structural breakdown of bentonite is potentially caused by radiation-induced amorphization through an ionization process.⁴¹ However, the ionizing effects should be carefully discussed with further studies, because amorphization dose is approximately 10^{10} – 10^{11} Gy which is significantly higher range than the γ -dose (i.e., $\sim 10^6$ Gy at 25 °C) used in this study.

Iodide Sorption Mechanism on SMB. Previous iodine sorption studies found that the iodine was covalently bound to carbon atoms composing the organic matter.^{30,35,37,42} Although organic surfactant was used for bentonite modification in this study, the FTIR spectra showed no C–I bonding at 660 cm^{-1} ⁴³ for all unirradiated and irradiated 200-SMB samples after the iodide sorption experiments. The observed bands of FTIR spectra for the iodide-loaded samples before and after the sorption experiments were similar regardless of the irradiation times (Figure 7c). In addition, XANES spectra of adsorbed iodide on 200-SMB without irradiation and 200-SMB after irradiation were identical each other (SI Figure S4). The XANES spectra of iodide adsorbed on SMB were also found to be very similar to the spectrum of KI reference. This suggests that the reduced form of iodine, iodide is predominant species on SMB after sorption and irradiation without the oxidation state change. Because iodide was not oxidized to form organo iodine on SMB, no strong chemical C–I bonding was found in FTIR analysis, which is different from our previous study of iodide sorption on black carbon.³⁰ Unfortunately, due to a poor signal-to-noise ratio, extended X-ray absorption fine structure (EXAFS) analysis was not conducted. Although further study may be necessary, these results above suggest that anionic iodide sorbs physically to the HDTMA on SMB by electrostatic attraction rather than by chemical binding of the iodide to the SMB.

Environmental Implication. The results of the iodide sorption experiments and SEM-EDS analyses indicated that the organic surfactant of HDTMA-Br on the SMB interacted with iodide. Although the iodide sorption capabilities of the SMB decreased slightly under high-temperature and/or irradiation conditions, the HDTMA-SMB developed in this study effectively sorbed iodide under alkaline conditions, such as those encountered by an engineered barrier surrounding a

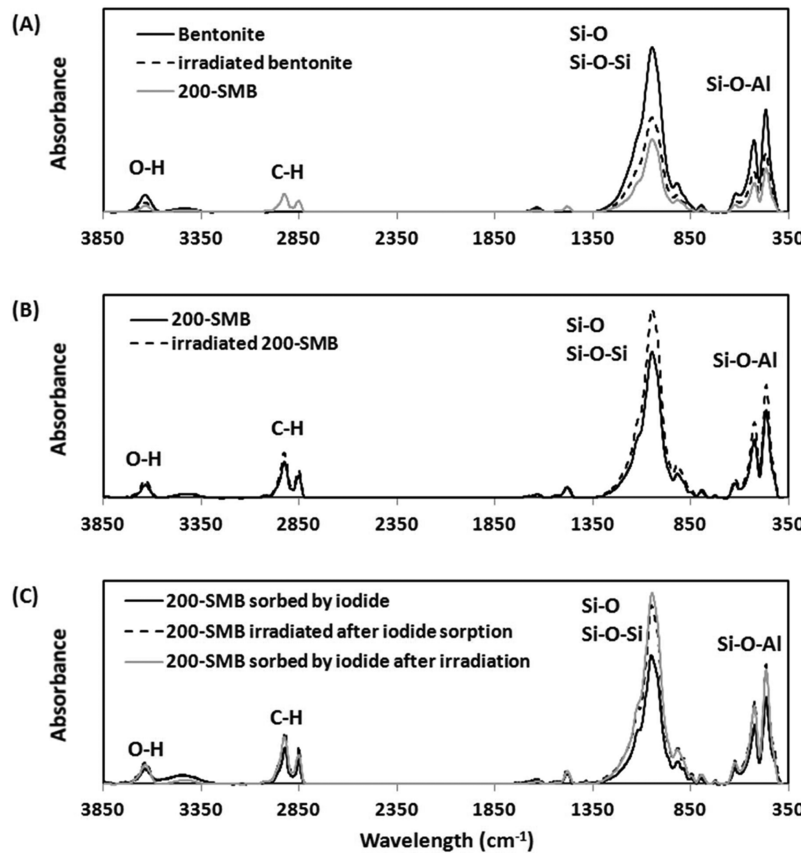


Figure 7. Comparison of FTIR spectra between (A) bentonite, irradiated bentonite, and 200-SMB, (B) 200-SMB and irradiated 200-SMB, and (C) 200-SMB sorbed by iodide, 200-SMB irradiated after iodide sorption, and 200-SMB sorbed by iodide after irradiation. The irradiated samples were prepared with a dose of 10^6 Gy using ^{60}Co source, and the iodide sorption experiments were conducted at high initial concentration of iodide, ~ 30 mg/L, for the FTIR analyses.

canister in a geological repository, and could be an effective sorbent for radioactive iodide remediation in the subsurface environment.

ASSOCIATED CONTENT

Supporting Information

The organic carbon fraction of the bentonite and SMB, related SEM-EDS data, iodide sorption results with different temperatures, and iodide XANES for 200-SMB and 200-SMB irradiated samples are provided in the Supporting Information. This material is available free of charge via the Internet at <http://pubs.acs.org>.

AUTHOR INFORMATION

Corresponding Author

*Phone: +1-509-372-6227; fax: +1-509-376-1638; e-mail: Wooyong.um@pnnl.gov.

Present Address

^VDivision of Earth and Environmental Science Research, Korea Basic Science Institute (KBSI), 162 Yeongudanji-ro, Ochang-eup, Cheongju 363-883, Republic of Korea.

Notes

The authors declare no competing financial interest.

ACKNOWLEDGMENTS

We especially appreciate the valuable and helpful comments of four anonymous reviewers. This research was supported by the BK21+ Program and Basic Science Research Program (NRF-

2012R1A1A2044287) through the National Research Foundation of Korea (NRF) funded by the Ministry of Education, Science, and Technology. Partial support was also provided by KBSI (Grant No.C34700). The study samples were irradiated at Advanced Technology Radiation Laboratory/KAERI, and the analyses of NMR and FTIR were conducted at KBSI. The XAFS spectra were collected at PAL and experiments at PLS were supported in part by MSIP and POSTECH.

REFERENCES

- (1) Zhang, S.; Du, J.; Xu, C.; Schwehr, K. A.; Ho, Y. F.; Li, H. P.; Roberts, K. A.; Kaplan, D. I.; Brinkmeyer, R.; Yeager, C. M.; Chang, H. S.; Santschi, P. H. Concentration-dependent mobility, retardation, and speciation of iodine in surface sediment from the Savannah River Site. *Environ. Sci. Technol.* **2011**, *45*, 5543–5549.
- (2) Balonov, M. The Chernobyl accident as a source of new radiological knowledge: Implications for Fukushima rehabilitation and research programmes. *J. Radiat. Prot.* **2013**, *33*, 27–40.
- (3) Frechou, C.; Calmet, D. ¹²⁹I in environment of the La Hague nuclear fuel reprocessing plant—from sea to land. *J. Environ. Radioact.* **2003**, *70*, 43–59.
- (4) Hou, X. L.; Malenchenko, A. F.; Kucera, J.; Dahlgaard, H.; Nielsen, S. P. Iodine-129 thyroid and urine in Ukraine and Denmark. *Sci. Tot. Environ.* **2003**, *302*, 63–73.
- (5) Franklyn, J. A.; Maisonneuve, P.; Sheppard, M. C.; Betteridge, J.; Boyle, P. Mortality after the treatment of hyperthyroidism with radioactive iodine. *N. Engl. J. Med.* **1998**, *338*, 712–718.
- (6) Vitti, P.; Delange, F.; Pinchera, A.; Zimmerman, M.; Dunn, J. T. Europe is iodine deficient. *Lancet* **2003**, *361*, 1226.

- (7) Um, W.; Serne, R. J.; Krupka, K. M. Linearity and reversibility of iodide adsorption on sediments from Hanford, Washington under water saturated conditions. *Water Res.* **2004**, *38*, 2009–2016.
- (8) Xu, C.; Miller, E. J.; Zhang, S.; Li, H.-P.; Ho, Y.-F.; Schwehr, K. A.; Kaplan, D. I.; Otosaka, S.; Roberts, K. A.; Brinkmeyer, R.; Yeager, C. M.; Santschi, P. H. Sequestration and remobilization of radioiodine (^{129}I) by soil organic matter and possible consequences of the remedial action at savannah river site. *Environ. Sci. Technol.* **2011**, *45*, 9975–9982.
- (9) Shetaya, W. H.; Young, S. D.; Watts, M. J.; Ander, E. L.; Bailey, E. H. Iodine dynamics in soils. *Geochim. Cosmochim. Acta* **2012**, *77*, 457–473.
- (10) Um, W.; Serne, R. J. Sorption and transport behavior of radionuclides in the proposed low-level radioactive waste disposal facility at the Hanford site, Washington. *Radiochim. Acta* **2005**, *93*, 57–63.
- (11) Kaplan, D. I.; Serne, R. J.; Parker, K. E.; Kutnyakov, I. V. Iodide sorption to subsurface sediments and illitic minerals. *Environ. Sci. Technol.* **2000**, *34*, 399–405.
- (12) Bors, J.; Dultz, S.; Riebe, B. Organophilic bentonites as adsorbents for radionuclides: I. Adsorption of ionic fission products. *Appl. Clay Sci.* **2000**, *16*, 1–13.
- (13) Riebe, B.; Dultz, S.; Bunnenberg, C. Temperature effects on iodine adsorption on organo-clay minerals: I. Influence of pretreatment and adsorption temperature. *Appl. Clay Sci.* **2005**, *28*, 9–16.
- (14) Krishna, B. S.; Murty, D. S. R.; Jai Prakash, B. S. Surfactant-modified clay as adsorbent for chromate. *Appl. Clay Sci.* **2001**, *20*, 65–71.
- (15) Xi, Y.; Frost, R. L.; He, H.; Kloprogge, T.; Bostrom, T. Modification of Wyoming montmorillonite surfaces using a cationic surfactant. *Langmuir* **2005**, *21*, 8675–8680.
- (16) Lee, S. Y.; Kim, S. J.; Chung, S. Y.; Jeong, C. H. Sorption of hydrophobic organic compounds onto organoclays. *Chemosphere* **2004**, *55*, 781–785.
- (17) de Paiva, L. B.; Morales, A. R.; Valenzuela Diaz, F. R. Organoclays: Properties, preparation and applications. *Appl. Clay Sci.* **2008**, *42*, 8–24.
- (18) Dies, J.; de las Cuevas, C.; Tarrasa, F.; Miralles, L.; Pueyo, J. J.; Santiago, J. L. Thermoluminescence response of heavily irradiated calcic bentonite. *Radiat. Prot. Dosim.* **1999**, *85*, 481–486.
- (19) Ewing, R. C.; Weber, W. J.; Clinard, F. W., Jr Radiation effects in nuclear waste forms for high-level radioactive waste. *Prog. Nucl. Energy* **1995**, *29*, 63–127.
- (20) Riebe, B.; Meleshyn, A. The role of compaction on the anion adsorption performance of temperature-pretreated organoclays under different atmospheres. In *Clays in Natural & Engineered Barriers for Radioactive Waste Confinement 4th International Meeting*, Nantes, France, 2010; pp 429–430.
- (21) Inglethorpe, S.; Morgan, D.; Highley, D. and Bloodworth, A. *Industrial Minerals Laboratory Manual: Bentonite*; British Geological Survey: Nottingham, UK, 1993.
- (22) Stern, E. A.; Newville, M.; Ravel, B.; Yacoby, Y.; Haskel, D. The UWXAFS analysis package: Philosophy and details. *Phys. B* **1995**, *208–209*, 117–120.
- (23) Shen, Y.-H. Removal of phenol from water by adsorption–flocculation using organobentonite. *Water Res.* **2002**, *36*, 1107–1114.
- (24) Wang, T.; Zhu, J.; Zhu, R.; Ge, F.; Yuan, P.; He, H. Enhancing the sorption capacity of CTMA-bentonite by simultaneous intercalation of cationic polyacrylamide. *J. Hazard. Mater.* **2010**, *178*, 1078–1084.
- (25) Zhu, L.; Chen, B. Sorption behavior of p-nitrophenol on the interface between anion–cation organobentonite and water. *Environ. Sci. Technol.* **2000**, *34*, 2997–3002.
- (26) Ikhtiyarova, G. A.; Ozcan, A. S.; Gok, O.; Ozcan, A. Characterization of natural- and organo-bentonite by XRD, SEM, FT-IR and thermal analysis techniques and its adsorption behavior in aqueous solutions. *Clay Miner.* **2012**, *47*, 31–44.
- (27) Xi, Y.; Ding, Z.; He, H.; Frost, R. L. Structure of organoclays - an X-ray diffraction and thermo-gravimetric analysis study. *J. Colloid Interface Sci.* **2004**, *277*, 116–120.
- (28) Lee, S. Y.; Cho, W. J.; Hahn, P. S.; Lee, M.; Lee, Y. B.; Kim, K. J. Microstructural changes of reference montmorillonites by cationic surfactants. *Appl. Clay Sci.* **2005**, *30*, 174–180.
- (29) Xi, Y. *Synthesis, Characterisation and Application of Organoclays*; Queensland University of Technology, 2006.
- (30) Choung, S.; Um, W.; Kim, M.; Kim, M.-G. Uptake mechanism for iodine species to black carbon. *Environ. Sci. Technol.* **2013**, *47*, 10349–10355.
- (31) Nilsson, K.; AB, G. *Hydrochemical Characterisation of Groundwater in the SFR Repository*; Swedish Nuclear Fuel and Waste Management Co.: Stockholm, 2011.
- (32) Pitkanen, P.; Snellman, M.; Vuorinen, U. *on the Origin and Chemical Evolution of Groundwater at the Olkiluoto site*; Posiva Oy: Helsinki, 1996.
- (33) Choi, B.-Y.; Kim, G.-Y.; Koh, Y.-K.; Shin, S.-H.; Yoo, S.-W.; Kim, D.-H. Geochemical characteristics of a LILW repository I. Groundwater. *J. Korean Radioact. Waste Soc.* **2008**, *6*, 297–306 (in Korean).
- (34) Schwarzenbach, R. P.; Gschwend, P. M.; Imboden, D. M. *Environmental Organic Chemistry*, 2nd ed.; John Wiley & Sons: Hoboken, NJ, 2003.
- (35) Schlegel, M. L.; Reiller, P.; Mercier-Bion, F.; Barre, N.; Moulin, V. Molecular environment of iodine in naturally iodinated humic substances: Insight from X-ray absorption spectroscopy. *Geochim. Cosmochim. Acta* **2006**, *70*, 5536–5551.
- (36) Schwehr, K. A.; Santschi, P. H.; Kaplan, D. I.; Yeager, C. M.; Brinkmeyer, R. Organo-iodine formation in soils and aquifer sediments at ambient concentrations. *Environ. Sci. Technol.* **2009**, *43*, 7258–7264.
- (37) Xu, C.; Zhong, J.; Hatcher, P. G.; Zhang, S.; Li, H.-P.; Ho, Y.-F.; Schwehr, K. A.; Kaplan, D. I.; Roberts, K. A.; Brinkmeyer, R.; Yeager, C. M.; Santschi, P. H. Molecular environment of stable iodine and radioiodine (^{129}I) in natural organic matter: Evidence inferred from NMR and binding experiments at environmentally relevant concentrations. *Geochim. Cosmochim. Acta* **2012**, *97*, 166–182.
- (38) Dultz, S.; Riebe, B.; Bunnenberg, C. Temperature effects on iodine adsorption on organo-clay minerals II. Structural effects. *Appl. Clay Sci.* **2005**, *28*, 17–30.
- (39) Senturk, H. B.; Ozdes, D.; Gundogdu, A.; Duran, C.; Soylak, M. Removal of phenol from aqueous solutions by adsorption onto organomodified Tirebolu bentonite: Equilibrium, kinetic and thermodynamic study. *J. Hazard. Mater.* **2009**, *172*, 353–362.
- (40) Sullivan, E. J.; Hunter, D. B.; Bowman, R. S. Fourier transform raman spectroscopy of sorbed HDTMA and the mechanism of chromate sorption to surfactant-modified clinoptilolite. *Environ. Sci. Technol.* **1998**, *32*, 1948–1955.
- (41) Allard, T.; Calas, G. Radiation effects on clay mineral properties. *Appl. Clay Sci.* **2009**, *43*, 143–149.
- (42) Xu, C.; Zhang, S.; Ho, Y.-F.; Miller, E. J.; Roberts, K. A.; Li, H.-P.; Schwehr, K. A.; Otosaka, S.; Kaplan, D. I.; Brinkmeyer, R.; Yeager, C. M.; Santschi, P. H. Is soil natural organic matter a sink or source for mobile radioiodine (^{129}I) at the Savannah River Site? *Geochim. Cosmochim. Acta* **2011**, *75*, 5716–5735.
- (43) Silverstein, R. M.; Webster, F. X.; Kiemle, D. *Spectrometric Identification of Organic Compounds*, 7th ed.; John Wiley & Sons, Inc.: Hoboken, 2005.